5-2015

Subsurface Fluid Flow Through the Mississippian Section of North-Central Oklahoma

Carolyn Brown
University of Arkansas, Fayetteville

Subsurface Fluid Flow through the Mississippian Section of North-Central Oklahoma

Subsurface Fluid Flow through the Mississippian Section
of North-Central Oklahoma

A thesis submitted in partial fulfillment
of the requirements for the degree of
Master of Science in Geology

by

Carolyn Brown
University of Arkansas
Bachelor of Science in Geology, 2013

May 2015
University of Arkansas

This thesis is approved for recommendation to the Graduate Council.

_____

Dr. Ralph Davis
Thesis Director

_____ _____

Dr. Matt Covington
Committee Member

Dr. Adriana Potra
Committee Member

Abstract

A Mississippian aged tripolitic chert reservoir located in Osage County, Oklahoma has been the target of conventional hydrocarbon exploration for many years. More recently companies have reinstated interest in the reservoir with the intentions of employing unconventional production processes. However, due to the nature of the karst formation, concerns have been raised about how the hydraulic fracturing fluids will affect the existing water system and how fluid flow in the formation will impact petroleum production.

This study consisted of using drill stem tests, seismic amplitude data, and well logs to create the parameters needed to construct a groundwater flow model for a portion of Osage County. At the start, a potentiometric map of Osage County, Oklahoma was generated to use as a basis for the initial hydraulic heads and the constant heads in the model. Next, three seismic amplitude images were produced in a seismic interpretation program, OpenDtect, to base the hydraulic conductivity values on. In addition, utilizing Gamma Ray on 12 separate wells east-west across the county, a structural cross-section was created within Petra. Last, all the parameters produced from the previous steps were input into Modflow to create three separate flow models, one being the calibrated model and the other two being the sensitivity analysis models. The final results establish a reliable method to produce the data parameters needed to successfully create a spatially larger model to accurately describe this systems controls on porosity and permeability and hence, the reservoir flow capabilities and quantities.

Acknowledgments

I would like to give a very gracious thank you to my committee, Dr. Ralph Davis, Dr. Matthew Covington, and Dr. Adriana Potra for their guidance and encouraging words throughout my project and helping me complete my graduate degree. I would also like to extend a special thank you to those who went above and beyond by helping me with programs and data acquisition, Dr. Christopher Liner, Dr. Edith Wilson, Ceja Corporation, and Kevin Liner. Lastly, a final thank you to anyone who listened to my frustrations and kept me going, every little gesture is greatly appreciated. Thank You.

Dedication

To Adilei and Lillian: without you two girls helping me to realize what I am truly capable of, I would have never made it to this point. Thank you for your understanding of the countless hours the computer was in my lap and all the times I was too busy or things were hectic. All of this was for the two of you and someday you'll be old enough to understand why I worked so incredibly hard. Always remember, I love you.

Table of Contents

List of Figures

I. Introduction

A Mississippian aged tripolitic chert reservoir located in Osage County, Oklahoma has been the target of conventional hydrocarbon exploration for many years. More recently companies have reinstated interest in the reservoir with the intentions of employing unconventional production processes. However, due to the nature of the karst formation, concerns have been raised about how the hydraulic fracturing fluids will affect the existing water system and how fluid flow in the formation will impact petroleum production.

Therefore, a fluid flow model will be beneficial in defining and highlighting the zones of high permeability and porosity, which could potentially allow for the highly saline groundwater fluids and/or the hydraulic fracturing fluids to penetrate into surrounding zones of the karstic system that may cause adverse effects on the groundwater system. In addition, the highlighted zones will allow for more efficient planning of the unconventional wells in the zones that are more viable due to properties that would lend towards higher production, as well as, location of larger reservoir zones.

By implementing hydrogeologic principals and mapping practices, the goal is to define karstic fluid flow throughout the reservoir, as well as, structural and stratigraphic controls on fluid flow. However, what makes this project so important and intriguing is that it is relatively unstudied, so in the process of this project and the future work that will be done, it is somewhat breaking ground on assessing and defining fluid flow in this dynamic karst system.

II. Hypotheses

There are at least two competing hypotheses related to paleothermal fluids movement within and through this formation, thus potentially affecting the hydrocarbon placement and migration, and facilitating mineralization associated with the Tri-State Mining District (McKnight 1979). However, the same two hypotheses are also related to the current fluids movement within this system and are highlighting the migration of the meteoric waters coming from the surface and the possible hydrocarbon movement, both being affected by the variations and spatial distribution of the porosity and permeability throughout the formation.

Within these units are existing fractures and faults resulting from the tectonic activities associated with the Ouachita Orogeny, the largest being multiple NE trending faults that exist to the basement (Poole et al., 2005). One of the hypotheses suggests that the paleo-thermal fluids that upwelled into the formations easily moved through the system along these major faults. Furthermore, the current meteoric fluids would percolate down from the surface and follow along these more permeable faults zones, allowing for weathering and alteration within these zones. In addition, there is also a secondary fracture system that runs perpendicular to the major faults that allows the fluids to penetrate deeper into the formations horizontally causing higher porosity and permeability across a broader area of the formation. This provides pathways for fluid to more easily move along existing bedding planes, further enhancing secondary permeability within the unit.. This leads to the rocks located close to the fracture and faults zones being highly affected, by having higher porosity and permeability, but the processes taper off deeper into the formations where the fluids cannot easily penetrate due to the very low matrix permeability of the rock (figure 1). This would lead to the driving of fluids, including

hydrocarbons, along the fractures and faults, but would also mean that as the rocks are affected, the hydrocarbons would push deeper into the newly formed higher permeable and porous formation zones. However, this would also mean that located deeper within the matrix block of the formation, where the thermal waters or meteoric fluids did not penetrate as easily, the reservoir would be original in-place hydrocarbons, as opposed to the other reservoirs consisting of migrated hydrocarbons.

The second hypothesis is that the altered and weathered zones are more horizontally planar, being formed by exposure due to transgression and regression of the seas over many different intervals (Mazzulo et al., 2011). Thus the more permeable and porous zones would be located on a horizontally broader, more regionally defined area with several separate layers. Meaning that the more penetrable reservoir would be located in these regionally defined planar exposure surfaces as opposed to more widespread vertical zones, with horizontal zones connecting in-between.

Although, considering that the faults and fractures do exist, it is reasonable to assume that there are fluids traveling along these penetrable fault paths causing weathering and dissolution, even if the second hypothesis is correct. Furthermore, in terms of time, the fluid dissolution occurring along the structural discontinuities has been occurring since the onset of the Ouachita Orogeny, when the faulting and fracturing transpired (Poole et al., 2005), and is still continuing, due to the meteoric fluids. Therefore, if a planar weathered surface is found to exist it would be secondary to that of the fault and fracture dissolution surfaces. Thus, the major permeable and porous zones will be located along these structural surfaces, no matter the correct hypothesis. However, in terms of location of a large reservoir for an unconventional well, it would be

reasonable to assume that one would want to locate the horizontal zones for a broad, regional, hydrocarbon reservoir, if the second hypothesis is found to be viable.

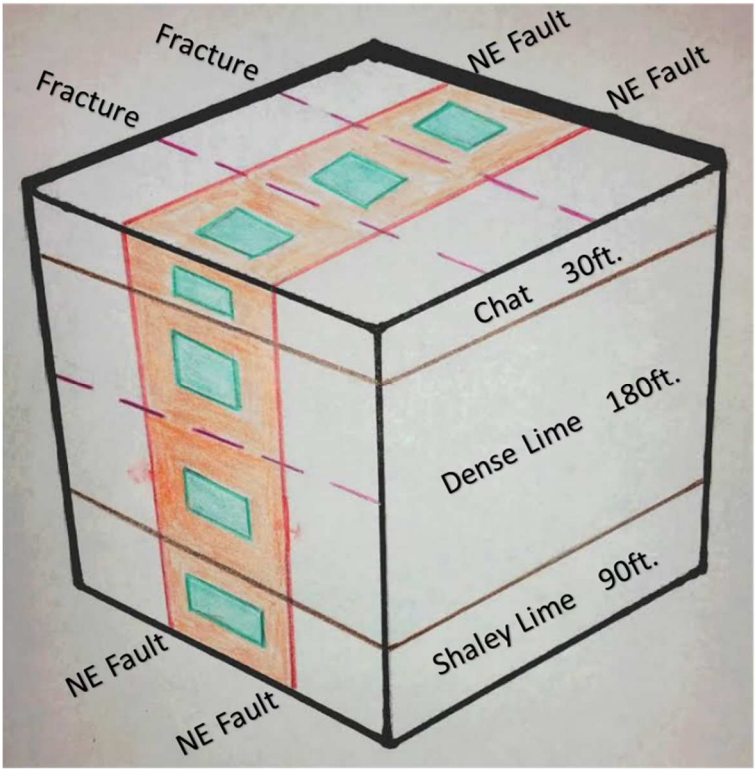

Figure 1: Conceptual Model of Mississippian block in North Central Oklahoma.

KEY:

NE trending faults: red lines.

Fracture system: pink dashes.

Formation sections: brown lines.

Area of infiltration and dissolution: orange.

Area of non-infiltration: green.

III. Depositional and Hydrogeologic History

3.1 Geologic Setting

Shallow seas covered the majority of Oklahoma during most of the first half of the Mississippian Period (Johnson, 2008). This area existed as a warm, shallow sea located on a carbonate platform at approximately 20 degrees south latitude (Watney et al., 2001) and is shown, outlined in a red box, on figure 2 from a modified image from Blakey (2013). This extensive shelf margin trended east-west along the Oklahoma-Kansas border (Watney et al., 2001) where Osage County, Oklahoma is found located on top of the Cherokee Platform and bounded to the west by the Nemaha Uplift and to the east by the Ozark Uplift (Johnson, 2008), as seen in figure 4.

3.2 Tectonic Setting

Tectonic activity began in the late Mississippian and continued into the Pennsylvanian (Rogers, 2001). Closure of a Paleozoic oceanic basin resulted in the Ouachita Orogeny (Leach et al., 1986), where the south-dipping subduction of the North-American Plate beneath a magmatic arc formed an accretionary wedge and resulted in a plate collision (Nelson et al., 1982; Viele, 1979). In the Neoproterozoic and Early Cambrian, the supercontinent Rodinia rifted along a NE-striking rift system and was later followed by the Ouachita orogenic belt faulting along this same rift system (Poole et al., 2005), allowing for the faulting, throughout much of the stratigraphic formations of this region, that exist into the basement.

3.3 Hydrogeologic Setting

By Middle Pennsylvanian time, the fluids recharging the system in the uplifted Ouachita foldbelt would be influenced by a gravity-driven hydraulic head created by the topographic relief with the resulting flow traveling northward out of the Arkoma basin (Leach et al., 1986). These rapidly flowing fluids were able to accomplish advective heat transfer where the observed temperatures appear to reflect the thermal gradient of a slowly cooling brine moving northward and subsequently resulted in the Mississippi Valley-type mineralization of the Tri-State Mining District (Leach et al., 1986). It is likely that these fluids resulted in significant weathering and dissolution of the limestone and chert adjacent to the large NE trending faults and also along the NW trending fracture sets that resulted from the orogeny. This ultimately resulted in zones of increased permeability within these zones relative to the lower permeability matrix blocks that the faults and fractures bound.

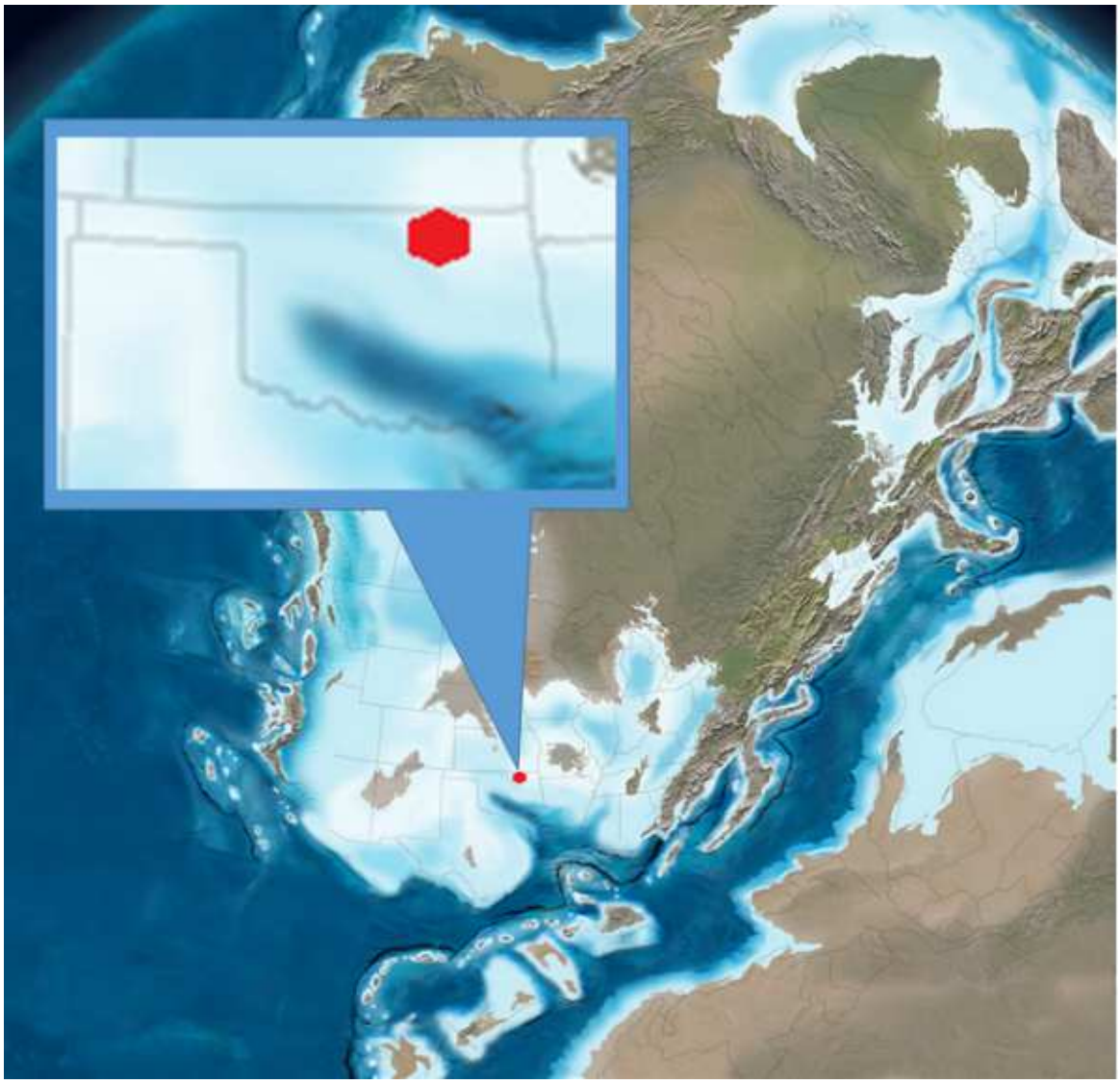

Figure 2: Depositional and Tectonic Setting During the Mississippian. Osage County, Oklahoma is indicated with the red dot. Modified from Blakey, 2013.

3.4 Stratigraphic Section

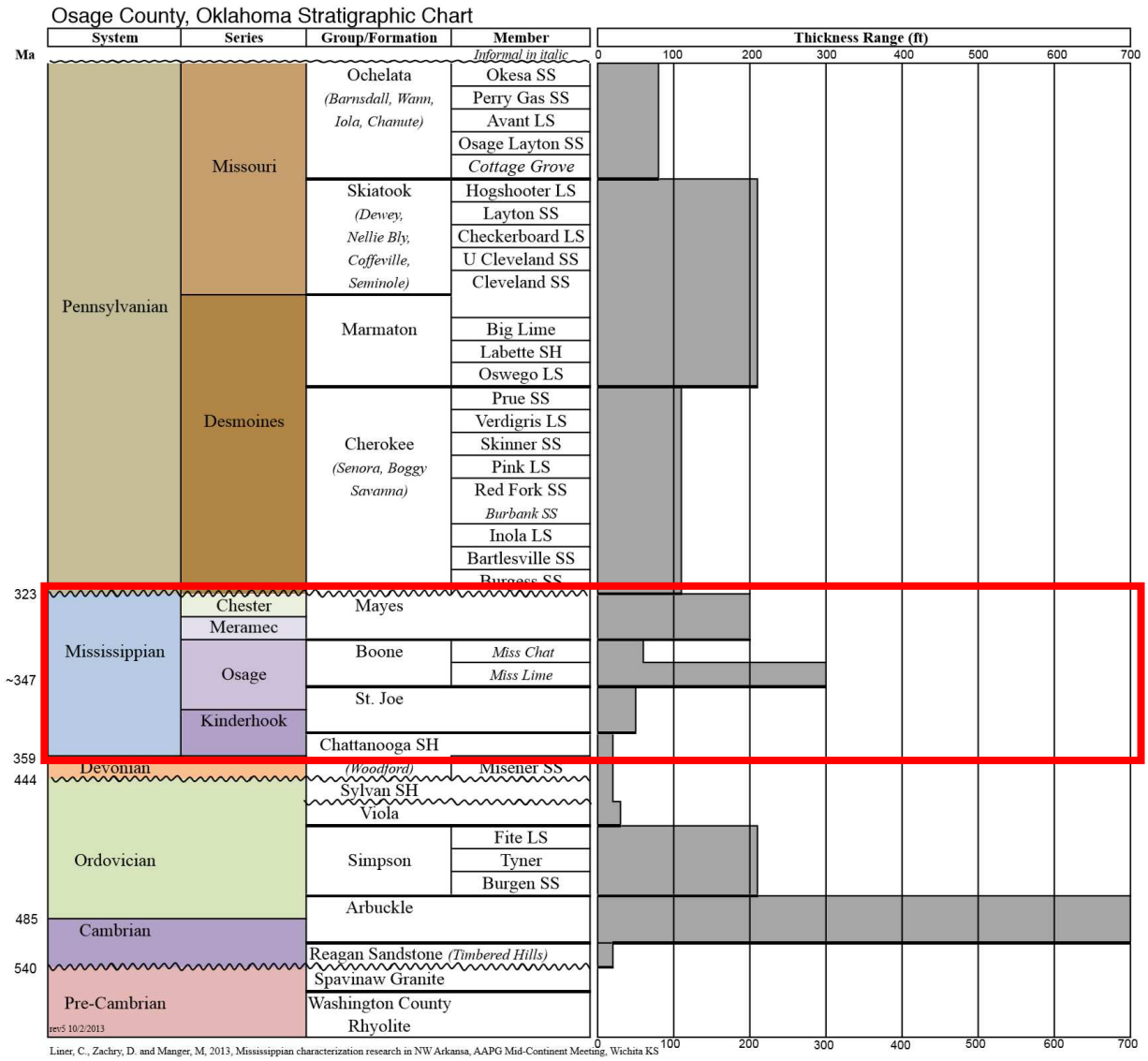

Figure 3: Osage County, Oklahoma stratigraphic section. Mississippian section of interest is highlighted with red box. Modified from Liner et al., 2013.

3.5 Structure of Osage County, Oklahoma

Osage County, Oklahoma is located on the Cherokee Platform, between the Nemaha Uplift to the west and the Ozark Uplift to the east and southeast as shown in Figure 5 (Johnson, 2008). To the southwest the county is bordered by the Anadarko Basin and to the south by the Arbuckle Mountains. However, there is no distinct border to the north, indicating this system extends northward into southern Kansas.

The Cherokee Platform is generally characterized by beds gently dipping to the west, with local folds and normal faults that retain some small relief with distinct northeast-southwest and northwest-southeast orientations (Rice, 1995). These structures appear to be basement-controlled and the relief on these structures increases with depth (Rice, 1995).

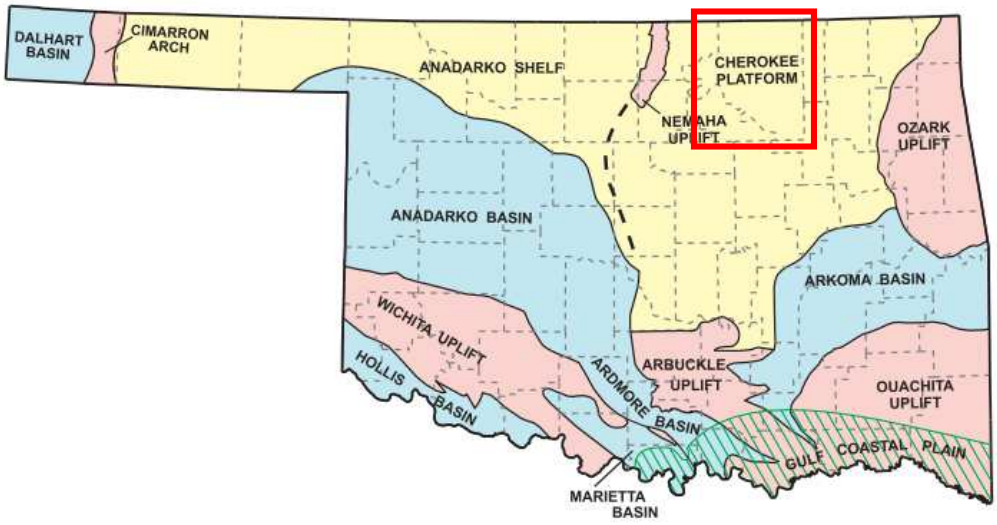

Figure 4: Current structural setting of the state of Oklahoma. Modified from Johnson, 2013. Area of study, Osage County, Oklahoma outlined in red.

IV. Methods

The project consisted of using well log data, drill stem tests and 3-D seismic data from the area to calculate the parameters needed to properly map the fluid dynamics and to construct the underground structure of the reservoir using Modflow and other relevant programs.

Objective 1: Within OpenDtect, a free open-source seismic interpretation software program, the seismic data from the Wild Creek Survey in Osage County, Oklahoma were flattened on the stratigraphically younger Pennsylvanian, Cherokee Horizon. To flatten the horizon, the top of the Mississippian Formation had to first be tracked in OpenDtect by manually picking this horizon across the domain of the seismic data and then using the auto-track function to create the full surface of the formation's top. Once this surface was successfully created, the topographic relief was flattened by hanging the elevation differences on the stratigraphically younger, Burbank Sandstone Formation, allowing for the relief to be flattened. Using this flattened horizon, three time slices were created and visually displayed using the grey scale color ramp. These three images created using this process highlight the changes in amplitude throughout the system and allow visualization of the slower velocity fractured areas that display lighter in the color scheme from that of the faster velocity areas that are denser to be differentiated from the darker less dense slower velocity zones. By highlighting the zones, the structure of the Mississippian block within the region was observable, and the spatially distributed amplitude data were used as a proxy for the spatial distribution of hydraulic conductivity throughout the domain. The amplitude data were used as the basis to assign hydraulic conductivity values for discrete zones within the 3D groundwater flow model. This

was limited to the Mississippian section between the Pennsylvanian Sandstone unit capping the Mississippian and the Woodford at the base.

The 3D Seismic amplitude data within Opendtect were converted to an x, y, z ascii grid that was uploaded into ImageJ, an open-source image processing program, to create the three images at 600 ms, 620 ms, and 634 ms. These seismic time-depths were converted to depths in feet using the conversion equation, $\Delta t = \frac{2\Delta z}{V}$, where Δt = the change in the seismic time, Δz = the change in the formation thickness, and v = velocity of the rock formation, so that for each image's seismic-time depth that the image was produced from could be converted to a depth in feet from the top of the formation, knowing that the top of the Mississippian Formation is close to 600ms. Thus indicating where the locations of the image slices are sited in feet, but also in a more general sense, the top of the formation, middle of the formation, and the lower portion of the formation, respectively. The amplitude images from ImageJ were re-gridded to contain pixel blocks equivalent to the node block size used for the Modflow model, 250ft x 250ft. Once the structure of the block had been established, the necessary hydraulic conductivities had to be estimated based on the higher to lower amplitudes. There are three ranges of hydraulic conductivity values estimated from tabulated data for hydraulic conductivity for various rock types (Freeze and Cherry, 1979): high, medium, and low in feet per second. For the high, the values range from $3\ x\ 10^{-4}$ to $3\ x\ 10^{-6}$, for the medium values $3\ x\ 10^{-6}$ to $3\ x\ 10^{-8}$, and lastly the low ranges, $3\ x\ 10^{-8}$ to $3\ x\ 10^{-10}$ $(all\ in \frac{feet}{second})$. This resulted in 7 different values for the hydraulic conductivities. Since the amplitudes range from 0-215, this allows for about 30 different $(\frac{215}{7} = 30.7)$ values within the amplitude set.

Objective 2: In order to calibrate the resulting flow models, a potentiometric map is required, with sufficient contouring of the data to provide quantitative comparison of observed vs modeled hydraulic head for each of the relevant zones. To complete the map, drill stem tests were acquired through multiple existing sources within the IHS database and files provided by Ceja Corporation. The specific values of the measuring depth datum, the final shut-in pressure, salinity, temperature and precise locations were pulled from these records. Using these data the total pressure head was calculated for each location. A total of 65 pressure head values were plotted and then contoured within Surfer to create the potentiometric map.

Relevant equations:

$$point\ Hp = \frac{P}{\rho w g}$$

point Hp = Point pressure head elevation

P = Final shut-in pressure

ρw = Calculated density of water due to known salinity

g = Acceleration due to gravity

$$P(calculated) = \rho w g(point\ Hp)$$

P = Pressure (calculated)

ρw = Calculated density of water due to known salinity

g = Acceleration due to gravity

$point\ Hp$ = point pressure head elevation

$$hp(fresh) = P(calculated)/\rho f g$$

hp(fresh) = Corrected pressure head elevation

P = Pressure (calculated)

ρf = Density of fresh water at observed well bore temperature

g = Acceleration due to gravity

Z + hp(fresh) = Pressure head elevation

Z = Drill Stem test depth

hp(fresh) = Corrected pressure head elevation

Objective 3: A structural cross section spanning east-west across Osage County, Oklahoma was created using Petra, by utilizing 12 wells with available Gamma Ray Curve. The potentiometric surface is also included on this structural cross-section, based on the head values calculated from the DST data and picks from the contoured potentiometric map. Once the cross section was completed, the potentiometric surface was drawn onto the map by locating the well on the potentiometric surface map and recording the correct elevation.

Objective 4: Using Modflow, a groundwater flow model of the Wild Creek Survey area (area location shown on Figure 9) plus 0.5 miles on either side, east to west and 0.25 miles north to south, was created. This made the total model area 10 miles x 5 miles. Within the modelling program a grid was created with the setup of 211 x 106 nodes (X,Y) with three layers, completing the Mississippian block at a total of 300 feet thick and making each node 250ft x 250ft. Once the grid setup was complete, the initial heads were input using polygons, which are manually created zones within the model domain using a polygon shape tool to draw them in. These values were pulled from the potentiometric surface map and input into the model using 3 different polygons to spatially distribute the initial heads across the model domain. Then the hydraulic conductivities were input, also using polygons, but since there are many more discrete ranges, a total of 42 polygons were needed. Next, the boundary condition, constant heads, were input using two separate polygons within each of the three zones of the formation. The elevation for the constant head for the eastern boundary is 1450 feet and the western boundary is 1200 feet, due to Modflow requiring the elevations of the formation block setup and the hydraulic heads to be positive, the potentiometric surface had to be converted from negative to positive values. These values are flattened and based on the top of the Mississippian, where the relief was flattened, based on the deepest depth of the formation in this specific area. Within Modflow the

formation block was setup as a total of 300 feet thick, setting the deepest subsea elevation in this area equal to 0 and the top of the formation to 300 feet. By doing so, the potentiometric surface elevations had to be altered to match the modeled block setup, so the elevation difference from the top of the actual formation depth to the potentiometric surface elevation was calculated and then the 300 feet of the modeled block was added to this value, resulting in the constant head elevations used in the model runs. For example, the eastern boundary depth, in the Wild Creek Survey area, to the top of the Mississippian Formation is close to -2050 feet and the potentiometric surface is close to -900 feet, resulting in a difference of 1150 feet between the two locations. Using that elevation difference and then adding 300 more feet to account for the entire model block (block is 300 feet thick), the final result for the model is 1450 feet. Lastly, the model was run using the solving criteria of LPF (layer property flow solving package), steady-state, 100 max iterations, and a head change criteria of 0.001 feet. Lastly a sensitivity analysis was run to determine the high and low values for hydraulic conductivity to where the model would no longer run to the closure criteria. These values are, for the high, $3.5\ x\ 10^{-4}\ to\ 3.5\ x\ 10^{-10}$ and for the low values, $1.5\ x\ 10^{-4}\ to\ 1.5\ x\ 10^{-10}$ in feet per second.

V. Results and Discussion

The three following images were produced to show the seismic amplitude structure and ranges to display the differences in the density properties of the rock. The darker colors indicate a higher density (higher velocity) and the lighter colors indicating lower density (lower velocity). The hydraulic conductivities were assigned based on the density, the more dense the rock, the lower the hydraulic conductivity, as shown with the darker colors and the higher conductivities, represented by the less dense rock is shown with lighter colors. The Wild Creek Survey area is 9 miles x 5 miles, so to create the full model area of 10 miles x 5 miles, the amplitude values had to be extrapolated to complete the model domain.

Objective 1: Amplitude to Hydraulic Conductivity

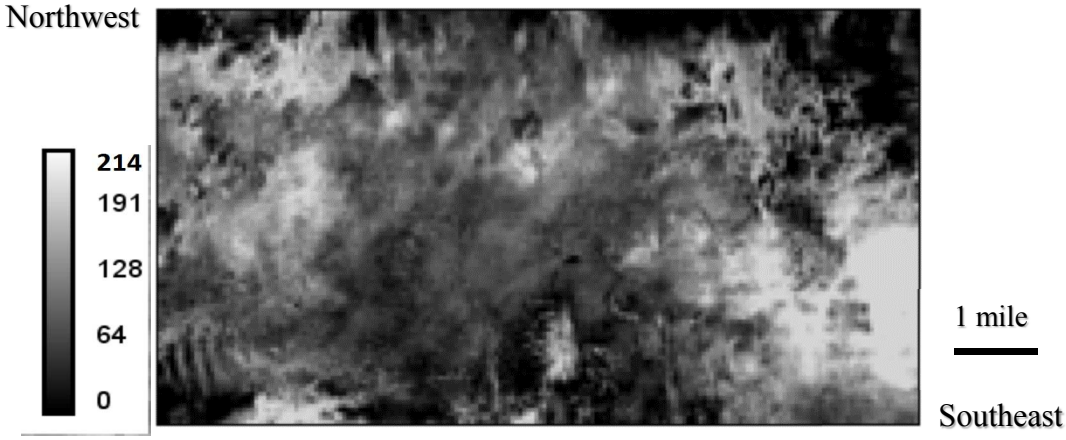

Figure 5: Amplitude structure of the top of the Mississippian Formation. For the model, this image represents the area at 300 feet within the model block.

(Seismic time-depth 600ms.)

Figure 6: Amplitude structure of the middle of the Mississippian Formation. For the model this image represents the area at 150 feet within the model block.

(Seismic time-depth 620ms.)

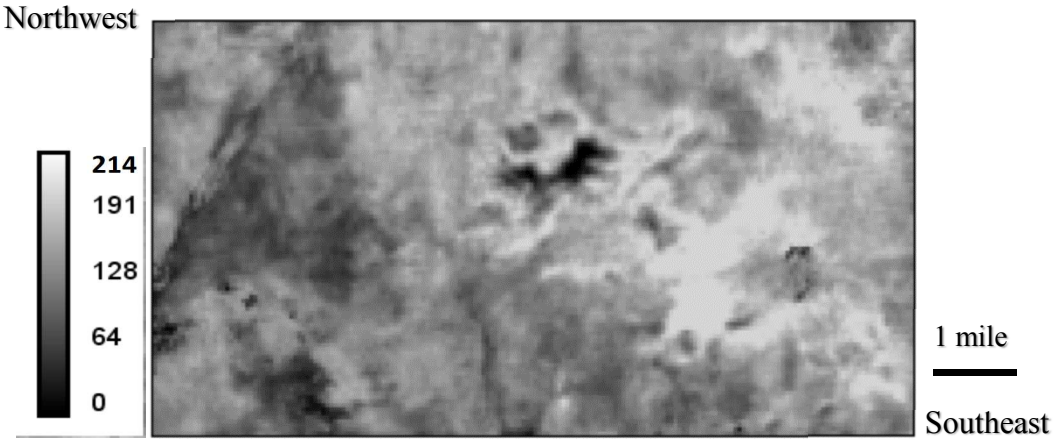

Figure 7: Amplitude structure of the lower portion of the Mississippian Formation.

For the model this image represents the area at 45 feet within the model block.

(Seismic time-depth 634ms)

Hydraulic Conductivity	Seismic Amplitude Range
3.28E-10	0-17
3.28E-09	18-35
3.28E-08	36-71
3.28E-07	72-107
3.28E-06	108-143
3.28E-05	144-179
3.28E-04	180-214

Figure 8: Seismic Amplitude Ranges with the estimated Hydraulic Conductivity ($\frac{ft}{s}$) Values shown used for Calibrated Model run.

For the Sensitivity Analysis runs, the values used were 1.5E-04 to 1.5E-10 ($\frac{ft}{s}$) for the lower range and for the higher range, 3.5E-04 to 3.5E-10 ($\frac{ft}{s}$).

Objective 2: Potentiometric Surface Map

The following images within objective 2 are the data and the results of the drill stem tests used to create the potentiometric map (Figures 9-13). The Google Earth image (Figure 9) displays the locations of the drill stem tests and are numbered to match to the tabulated data, shown in figure 10. These data were used to calculate the elevations of the potentiometric surface, to create the maps and structural diagrams (Figures 11-13). Figures 11 and 12 are the potentiometric surface maps, figure 11 has the contoured potentiometric elevations overlain onto a map of Osage County, Oklahoma. Figure 13 is the structural layout of the potentiometric surface, contoured to show the elevations on the surface.

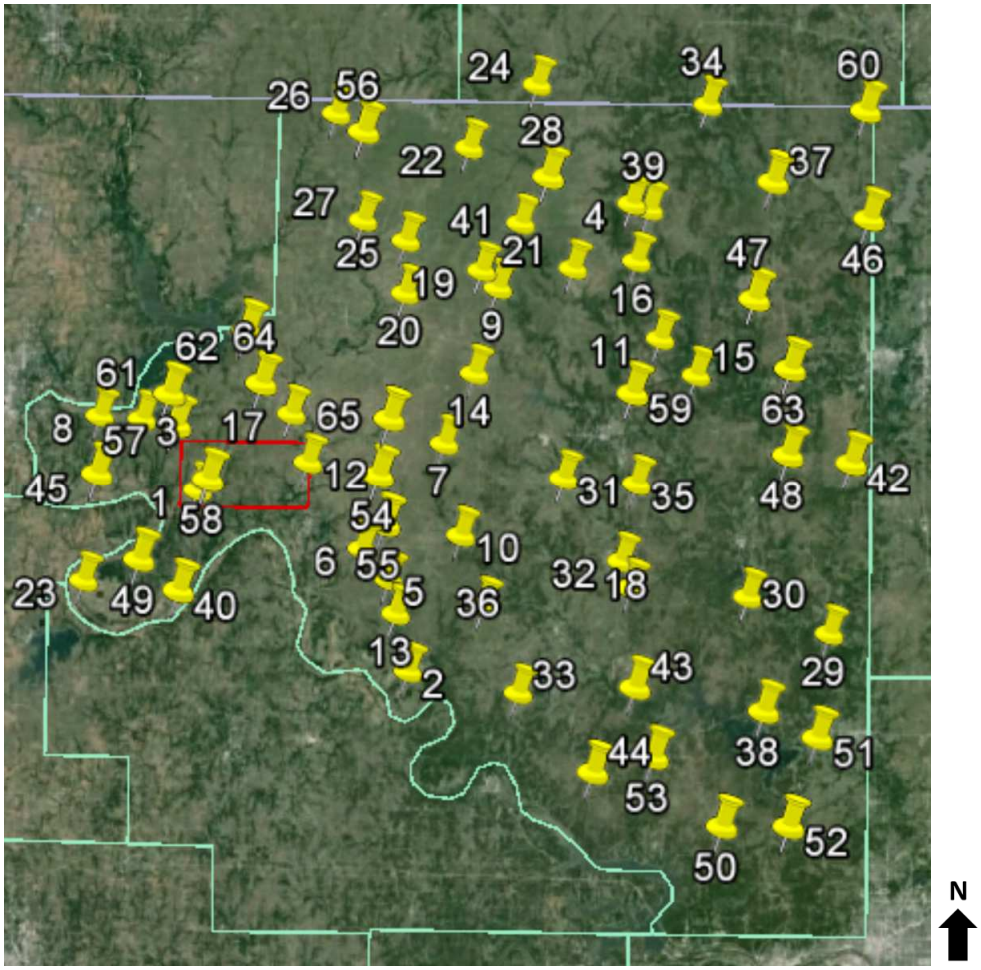

Figure 9: Google Earth image of Osage County, Oklahoma. Location of well drill stem tests, 65 total. Wild Creek survey outlined in red rectangle.

DST #	Corrected Pressure Head Elevation (ft)
1	-1138
2	-764
3	-1079
4	7
5	-787
6	-951
7	-469
8	-1325
9	-131
10	-512
11	-167
12	-941
13	-843
14	-522
15	-200
16	-161
17	-830
18	-489
19	-374
20	-636
21	-302
22	-121
23	-1745
24	-167
25	-387
26	-305
27	-2520
28	56
29	138
30	141
31	-266
32	-512
33	-886
34	36
35	-446
36	-390
37	16
38	-269
39	387
40	-1332
41	-92
42	59
43	-208
44	-210
45	-1325
46	26
47	-82
48	95
49	-1332
50	-512
51	-269
52	-561
53	-731
54	-551
55	-797
56	-463
57	-374
58	-1282
59	-289
60	-89
61	-1066
62	-705
63	151
64	-883
65	-436

Figure 10: Table of corrected pressure head elevations used to create the potentiometric surface map. DST # locations on Google Earth Image (Figure 8)

Figures 11 and 12 are the potentiometric surface maps, figure 11 has the contoured potentiometric elevations overlain onto a map of Osage County, Oklahoma. As shown in the maps, the potentiometric surface indicates that the flow is running from the east to the southwest, essentially flowing along the gradient dip of the Mississippian Formation to the west. The contours indicate not only the elevations of the potentiometric surface, but also indicate the structure and changes of the hydraulic conductivities. The large open spaced contours near the center of Osage County would indicate an area of higher hydraulic conductivity, while the more closely spaced contours just east and west of the Wild Creek block would represent areas of lower hydraulic conductivity.

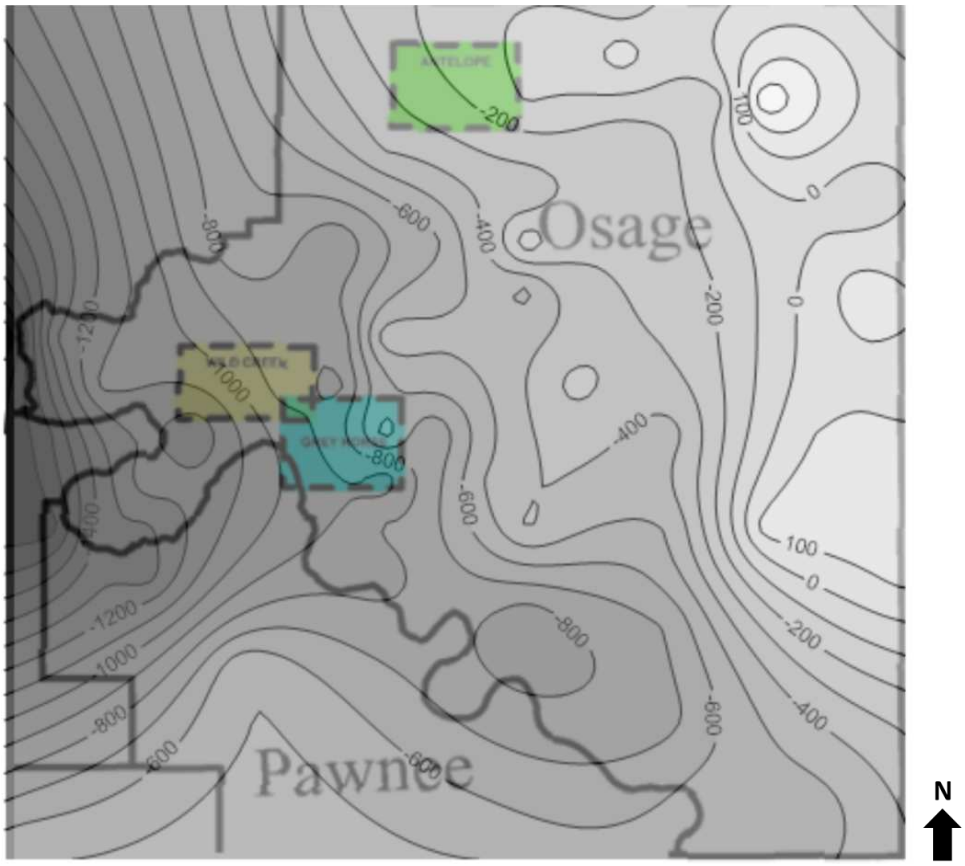

Figure 11: Potentiometric surface overlay on top of Osage County Map. Elevations in feet.

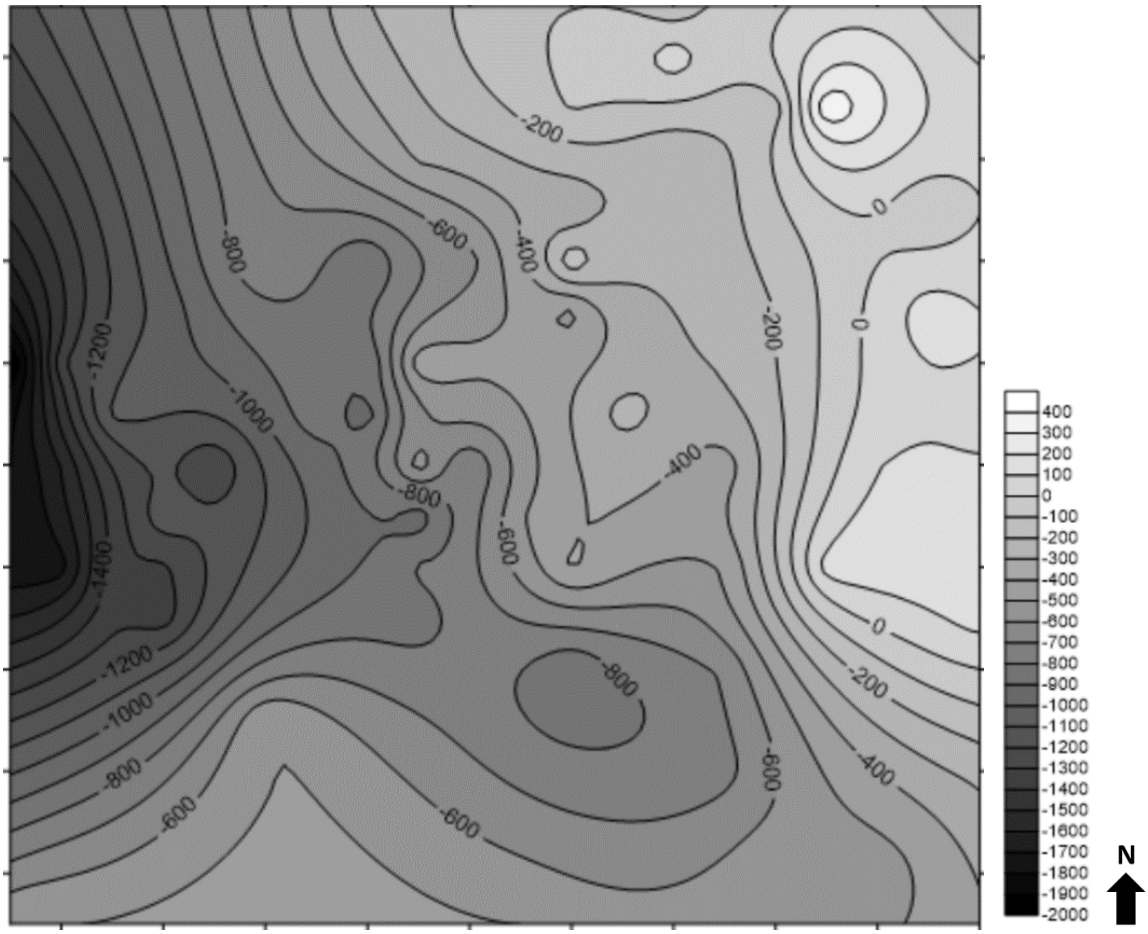

Figure 12: Potentiometric surface with color bar. Elevations in feet.

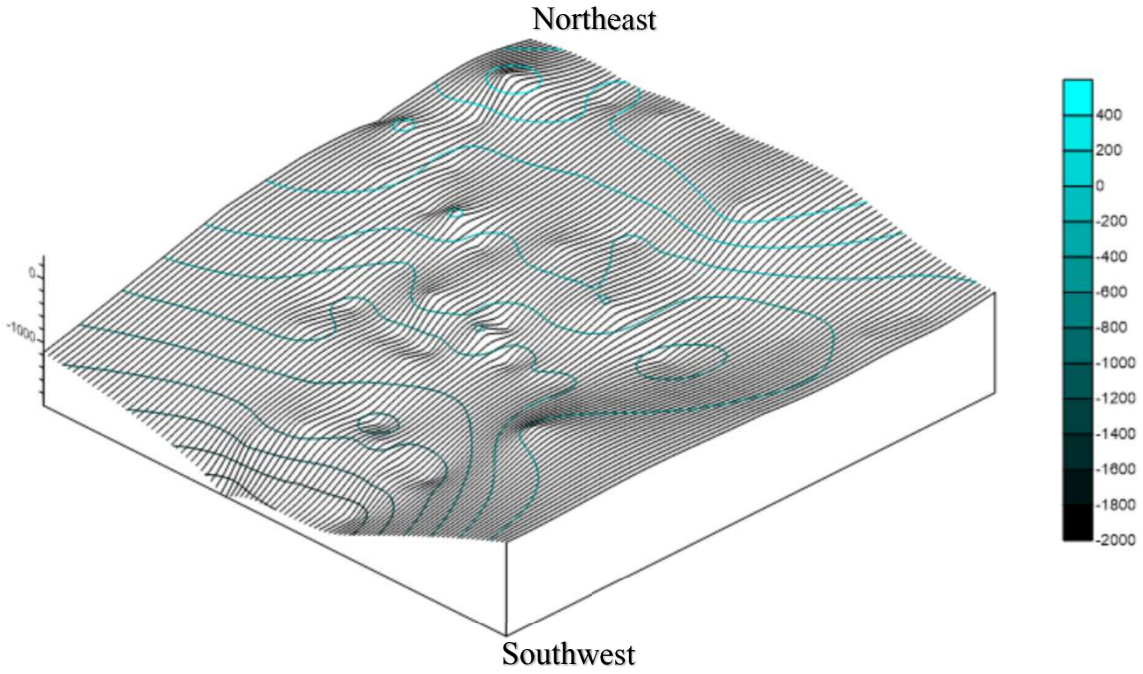

Figure 13: Structure of the potentiometric surface. Elevations in feet.

Objective 3: Structural Cross-Section

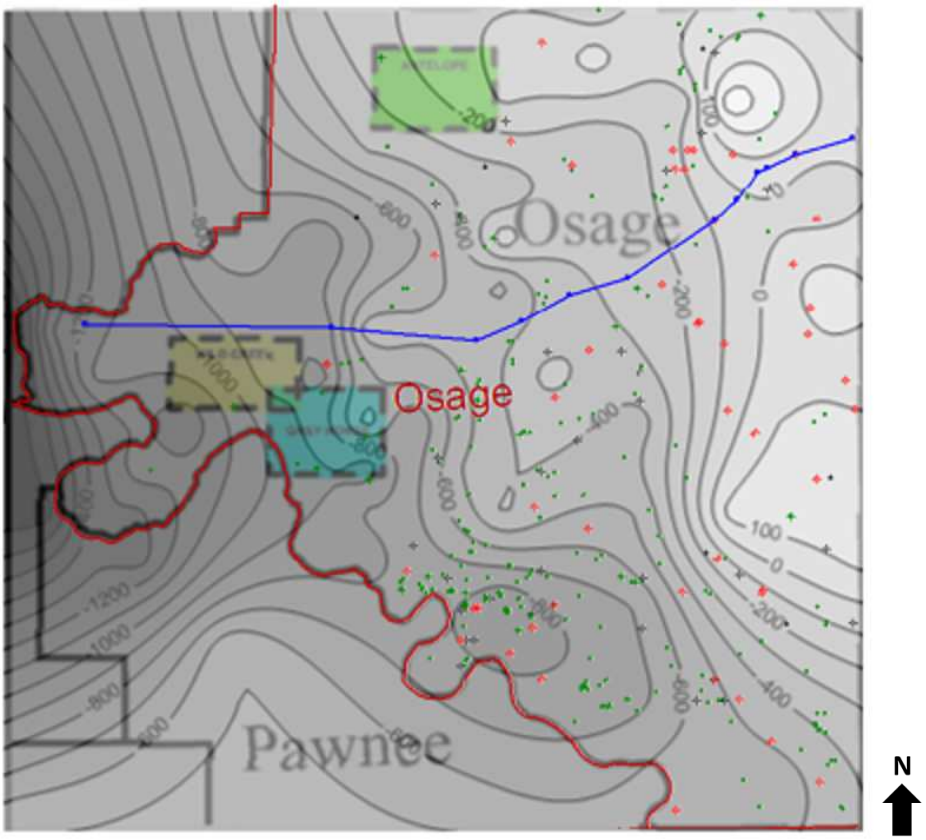

Figure 14: Cross-Section line shown in blue over potentiometric surface overlay on map of Osage County. Green spots indicate oil producing wells and red spots indicate natural gas producing wells.

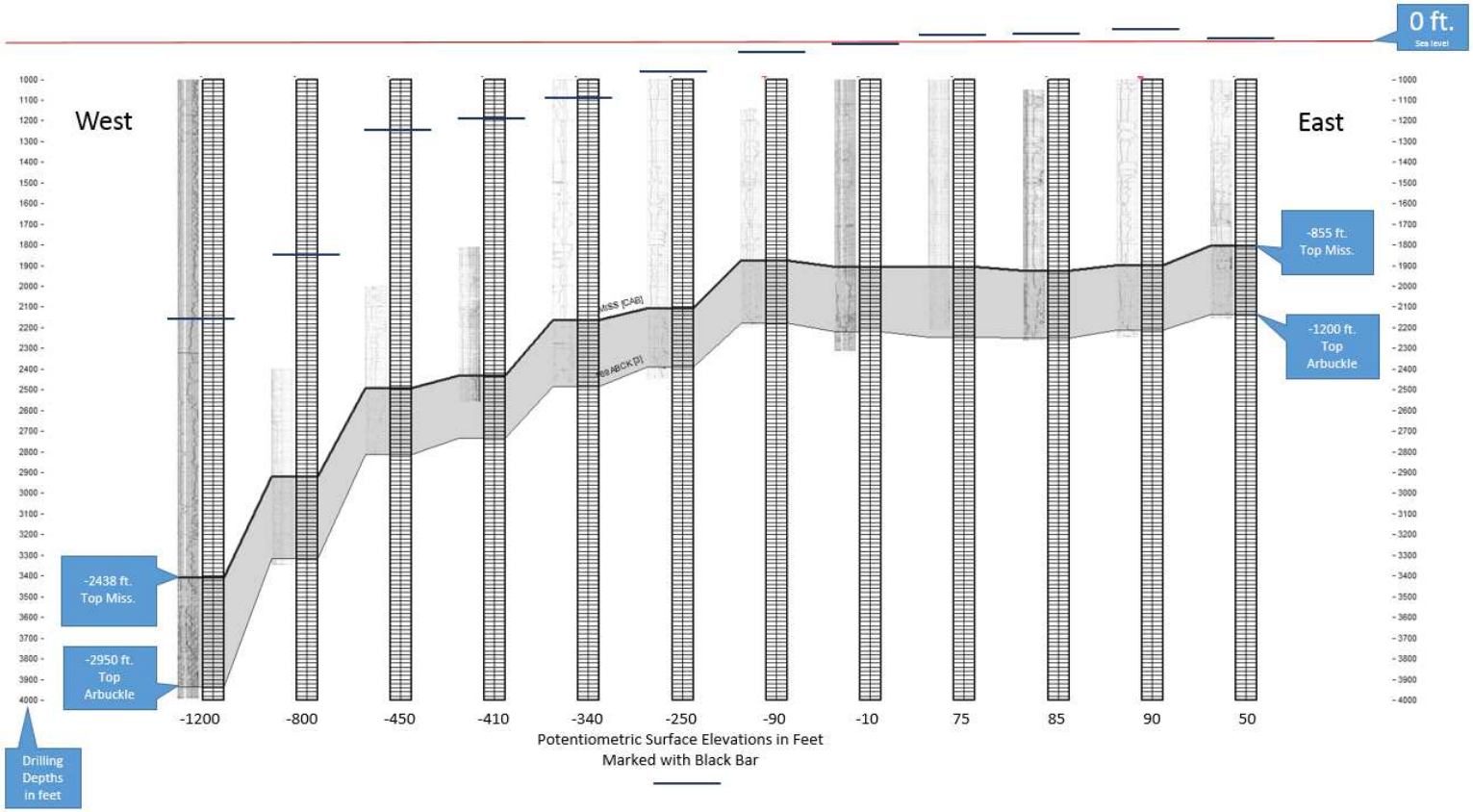

Figure 15: Cross-Section of the Mississippian Formation. Formation is shown in grey shading with the top marked with a thick black line. The bottom has been picked as the top of the stratigraphically younger Arbuckle formation, shown with a thin black line.

Objective 4: 3D Groundwater Flow Model

Objective 4 contains the final sets of images, consisting of the Modflow groundwater flow models with linear regressions of observed vs calculated heads, as well as, some of the setup parameters. Figures 17-20 show the maps of the polygons of the hydraulic conductivity values for each respective layer within the model block and a table displays the corresponding hydraulic conductivity values. Figures 21-24 are the calibrated model run and display each layer of the model block's hydraulic head map, indicating the fluid flow from the east to the west across the model domain. Figure 24 is the linear regression of the calibrated model run, using the potentiometric surface data from 10 wells in and within the immediate vicinity of the Wild Creek Survey area, as indicated with the yellow pins and the corresponding drill stem test number on figure 16.

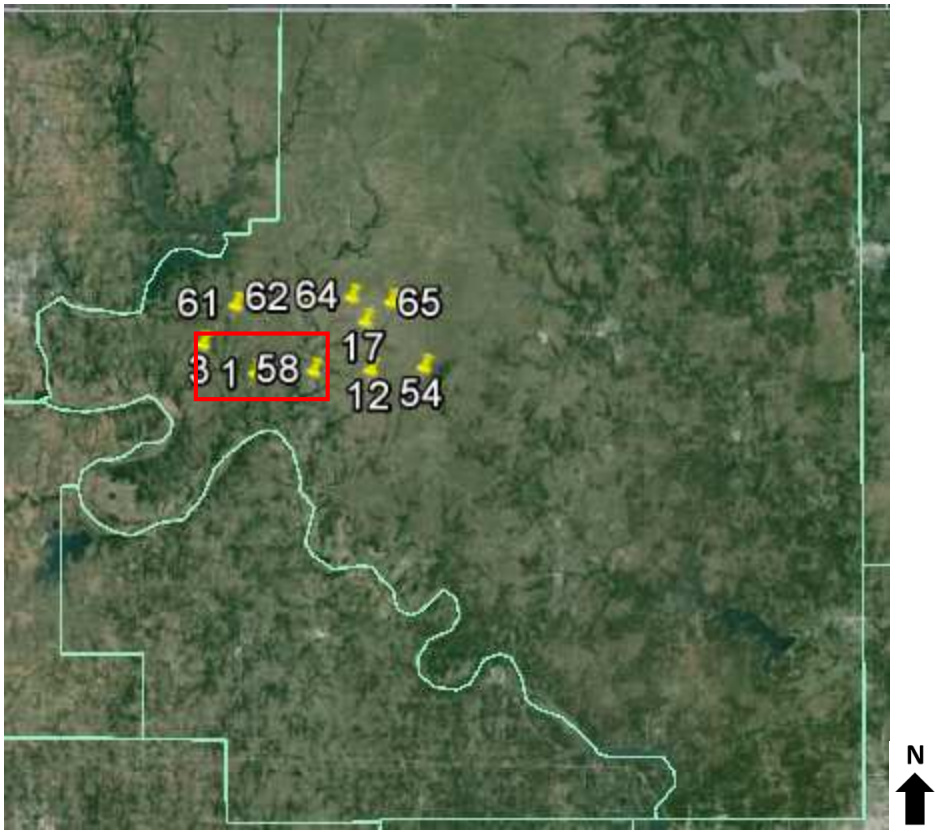

Figure 16: Google Earth Image of Osage County, Oklahoma. Wild Creek Survey Area Outlined with the Red Rectangle and the Locations of the Potentiometric Elevations used for the Linear Regressions of Observed vs Calculated Heads, Marked with the Pins with the Correlating Drill Stem Test Number

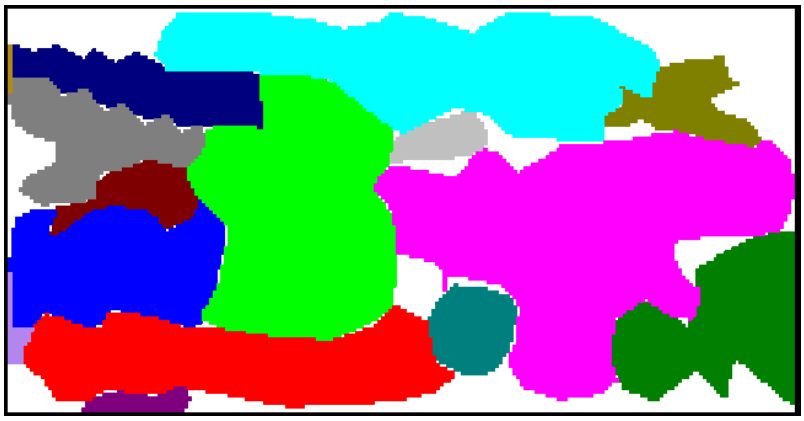

Figure 17: Layer 1 Hydraulic Conductivity Polygon Setup for Modflow Models

Figure 18: Layer 2 Hydraulic Conductivity Polygon Setup for Modflow Models

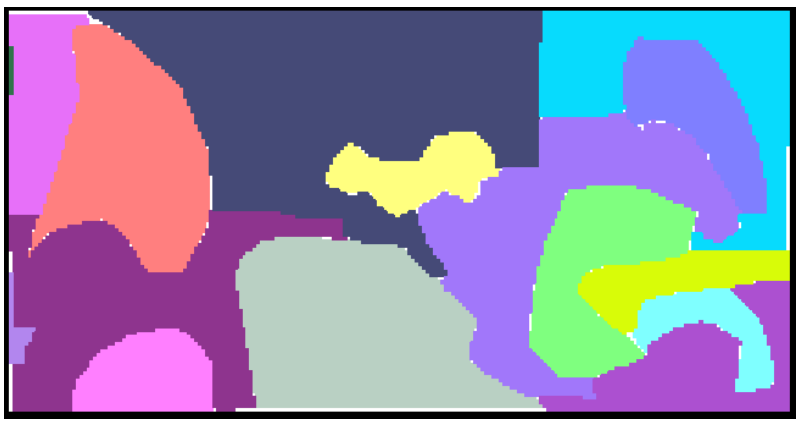

Figure 19: Layer 3 Hydraulic Conductivity Polygon Setup for Modflow Models

Zone	Color	Kx	Ky	Kz
1		3.28E-10	3.28E-10	3.28E-10
2		0.000328	0.000328	0.000328
3		0.000328	0.000328	0.000328
4		0.000328	0.000328	0.000328
5		0.000328	0.000328	0.000328
6		0.000328	0.000328	0.000328
7		0.000328	0.000328	0.000328
8		0.000328	0.000328	0.000328
9		3.28E-06	3.28E-06	3.28E-06
10		3.28E-06	3.28E-06	3.28E-06
11		3.28E-08	3.28E-08	3.28E-08
12		3.28E-08	3.28E-08	3.28E-08
13		3.28E-09	3.28E-09	3.28E-09
14		3.28E-09	3.28E-09	3.28E-09
15		3.28E-08	3.28E-08	3.28E-08
16		3.28E-08	3.28E-08	3.28E-08
17		3.28E-08	3.28E-08	3.28E-08
18		3.28E-05	3.28E-05	3.28E-05
19		3.28E-10	3.28E-10	3.28E-10
20		3.28E-10	3.28E-10	3.28E-10
21		3.28E-07	3.28E-07	3.28E-07
22		3.28E-07	3.28E-07	3.28E-07
23		3.28E-07	3.28E-07	3.28E-07
24		3.28E-07	3.28E-07	3.28E-07
25		0.000328	0.000328	0.000328
26		0.000328	0.000328	0.000328
27		0.000328	0.000328	0.000328
28		3.28E-09	3.28E-09	3.28E-09
29		3.28E-10	3.28E-10	3.28E-10
30		3.28E-10	3.28E-10	3.28E-10
31		3.28E-07	3.28E-07	3.28E-07
32		3.28E-06	3.28E-06	3.28E-06
33		3.28E-06	3.28E-06	3.28E-06
34		3.28E-06	3.28E-06	3.28E-06
35		3.28E-06	3.28E-06	3.28E-06
36		3.28E-06	3.28E-06	3.28E-06
37		3.28E-06	3.28E-06	3.28E-06
38		3.28E-06	3.28E-06	3.28E-06
39		3.28E-06	3.28E-06	3.28E-06
40		3.28E-05	3.28E-05	3.28E-05
41		3.28E-06	3.28E-06	3.28E-06
42		0.000328	0.000328	0.000328

Figure 20: Hydraulic Conductivity Values for Polygons on Calibrated Model Run, Sensitivity Analysis Used Same Polygons, but Their Respective Hydraulic Conductivity Values

Calibrated Model Run

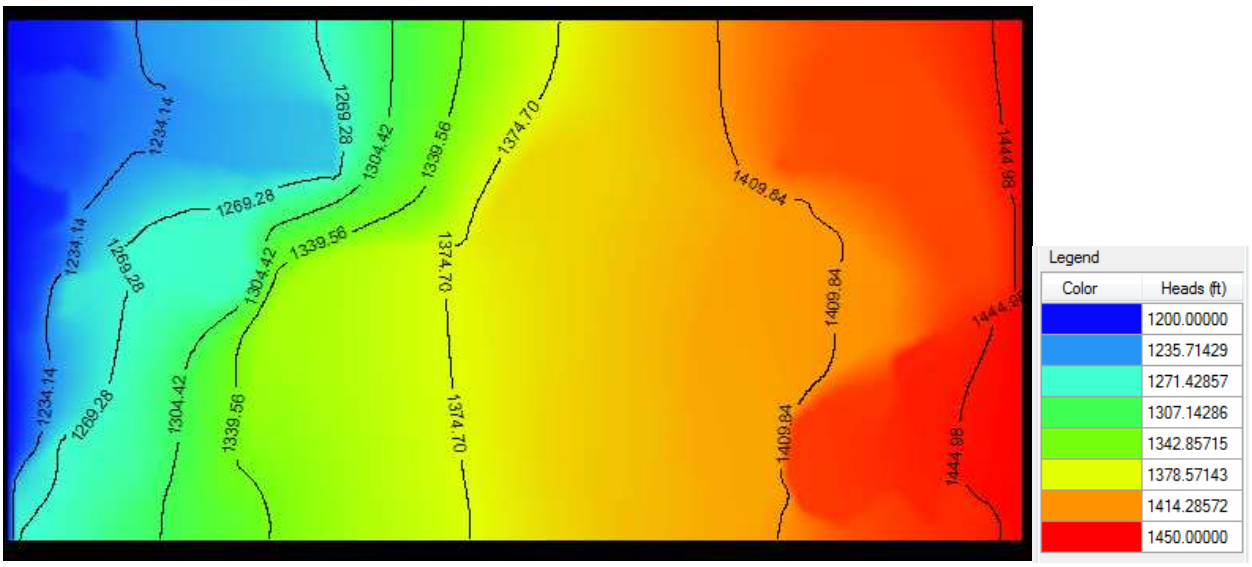

Figure 21: Calibrated Model Run, Layer 1

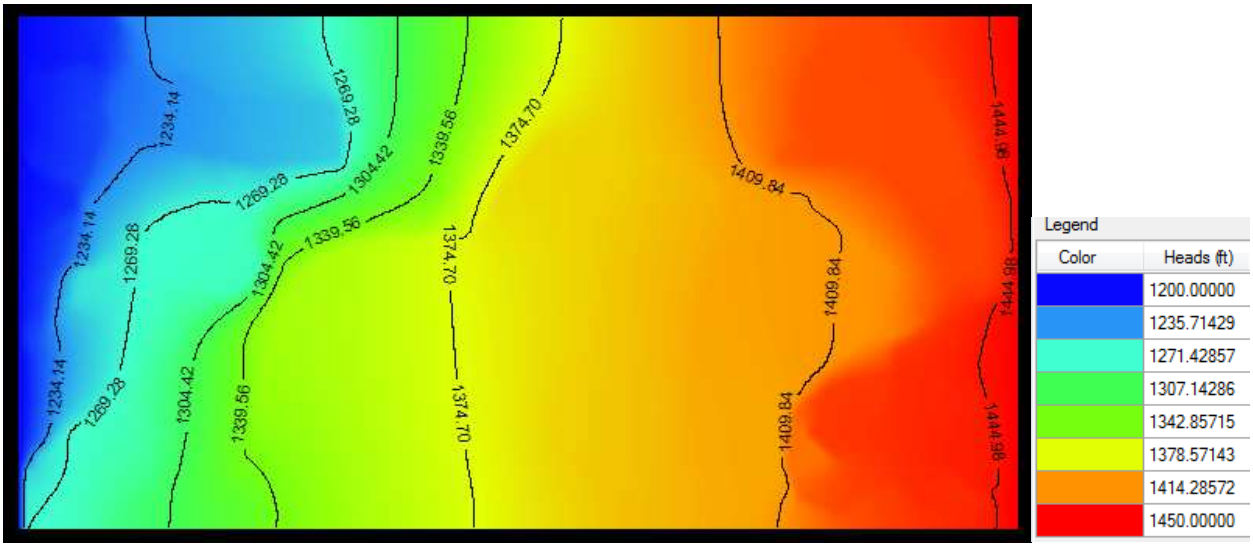

Figure 22: Calibrated Model Run, Layer 2

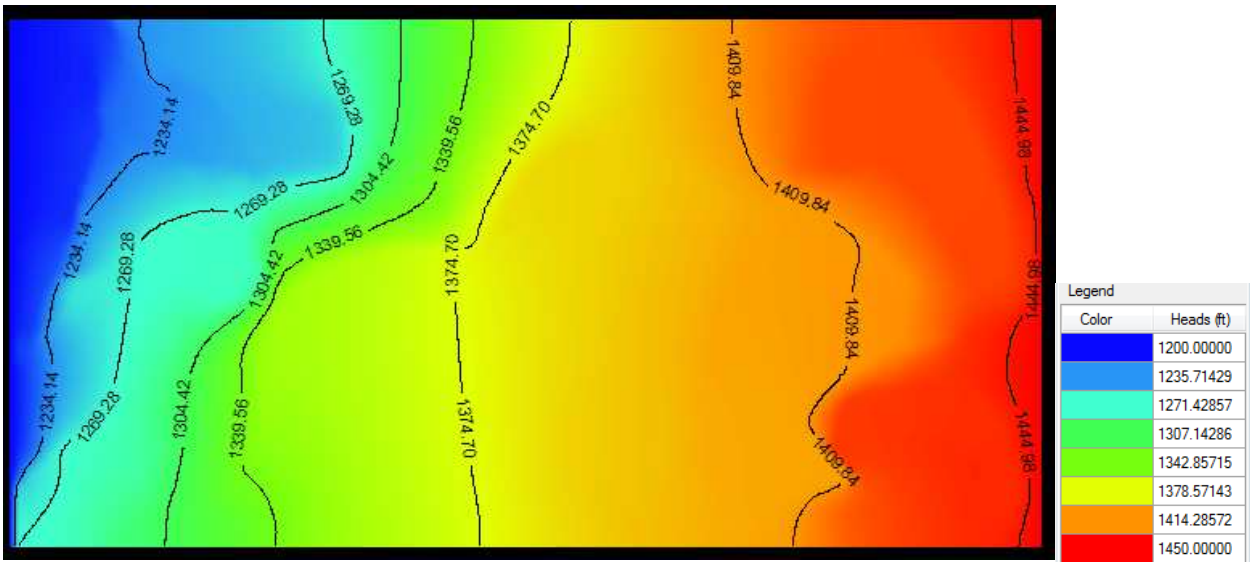

Figure 23: Calibrated Model Run, Layer 3

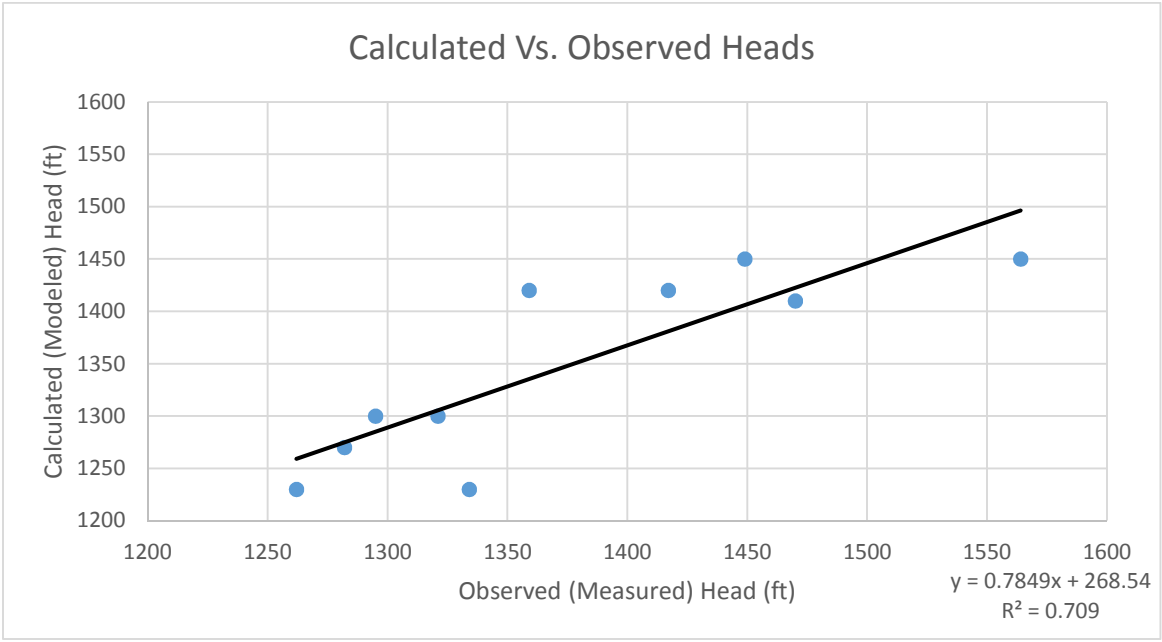

Figure 24: Linear Regression of Observed vs Calculated Heads on Calibrated Model Run, Layer 1

Sensitivity Analysis

Figures 25-32 show the sensitivity analysis's resulting hydraulic head maps for each respective layer. Two separate sets of hydraulic conductivities were input for the analysis, a lower range of 1.5E-04 to 1.5E-10 ($\frac{ft}{s}$) and for the higher range, 3.5E-04 to 3.5E-10 ($\frac{ft}{s}$). Linear regressions done for each of the sensitivity analysis runs indicated that they do not converge as closely to the potentiometric surface elevations as the calibrated model run.

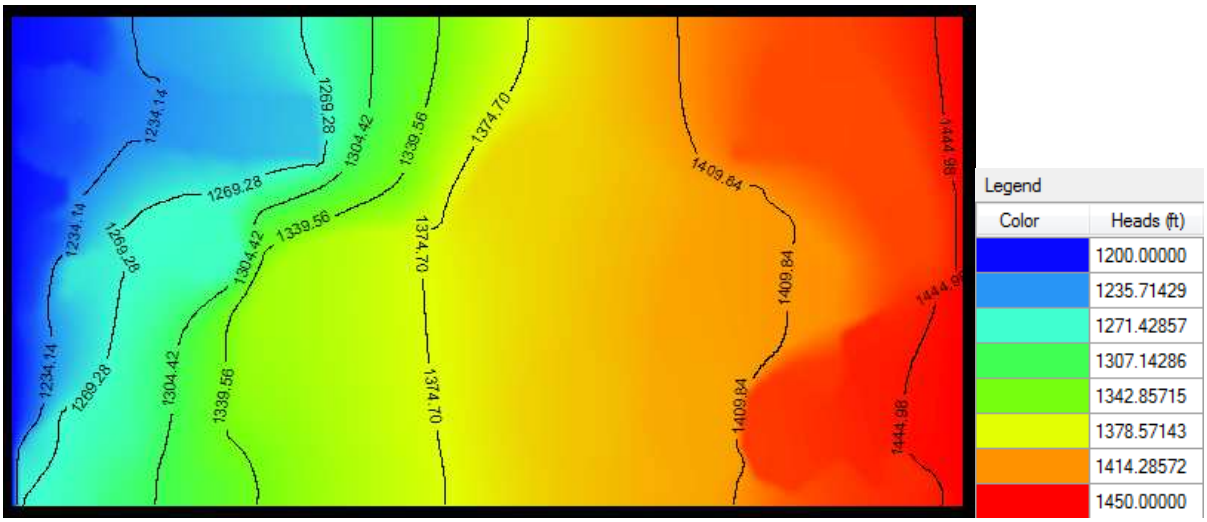

Figure 25: Sensitivity Analysis High Values, Layer 1, 3.5E-04 to 3.5E-10 ($\frac{ft}{s}$).

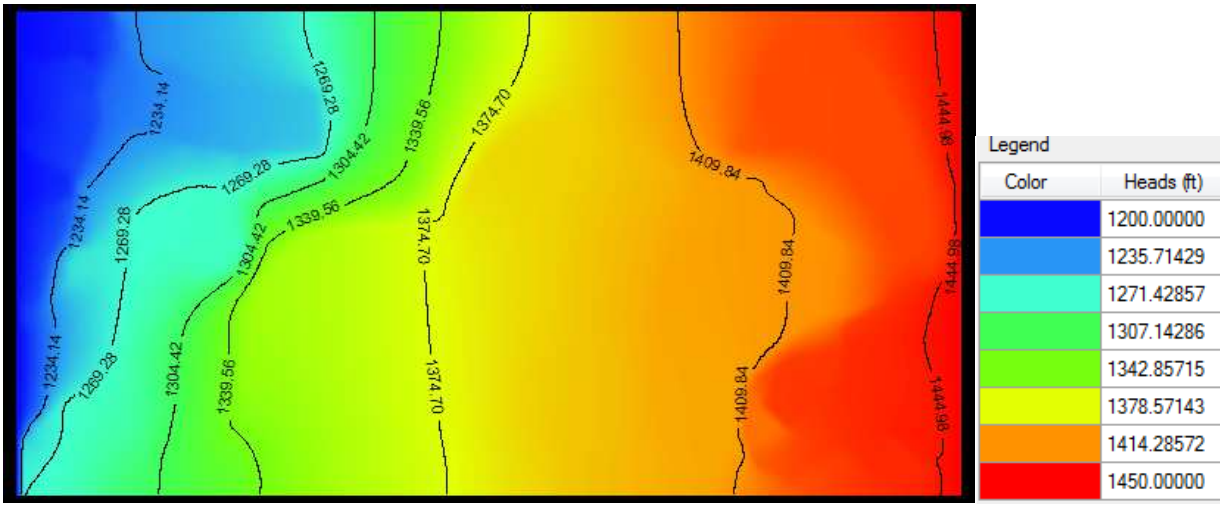

Figure 26: Sensitivity Analysis High Values, Layer 2, 3.5E-04 to 3.5E-10 ($\frac{ft}{s}$)

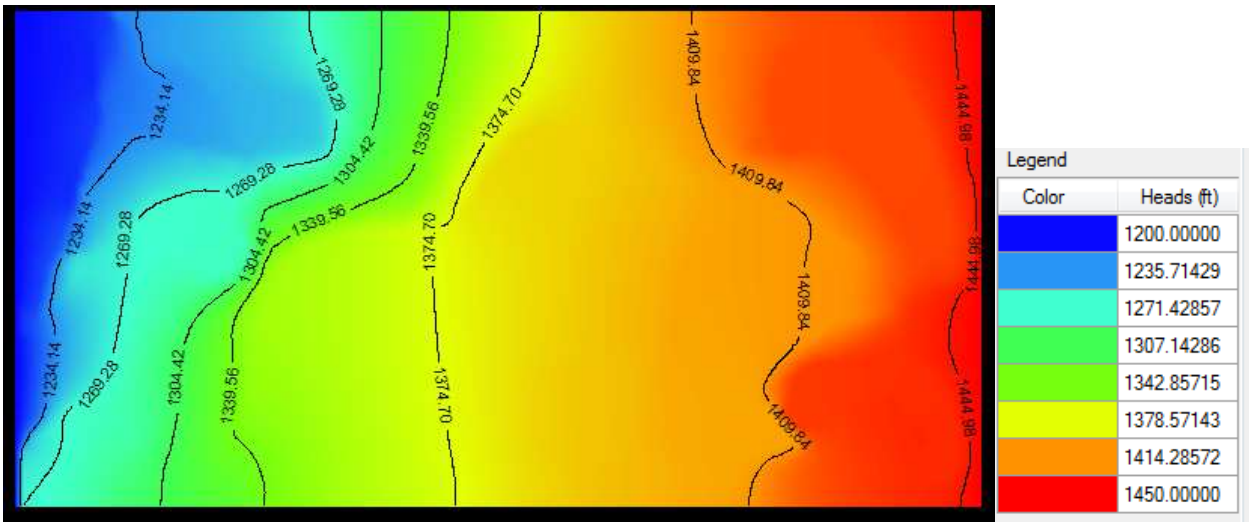

Figure 27: Sensitivity Analysis High Values, Layer 3, 3.5E-04 to 3.5E-10 ($\frac{ft}{s}$)

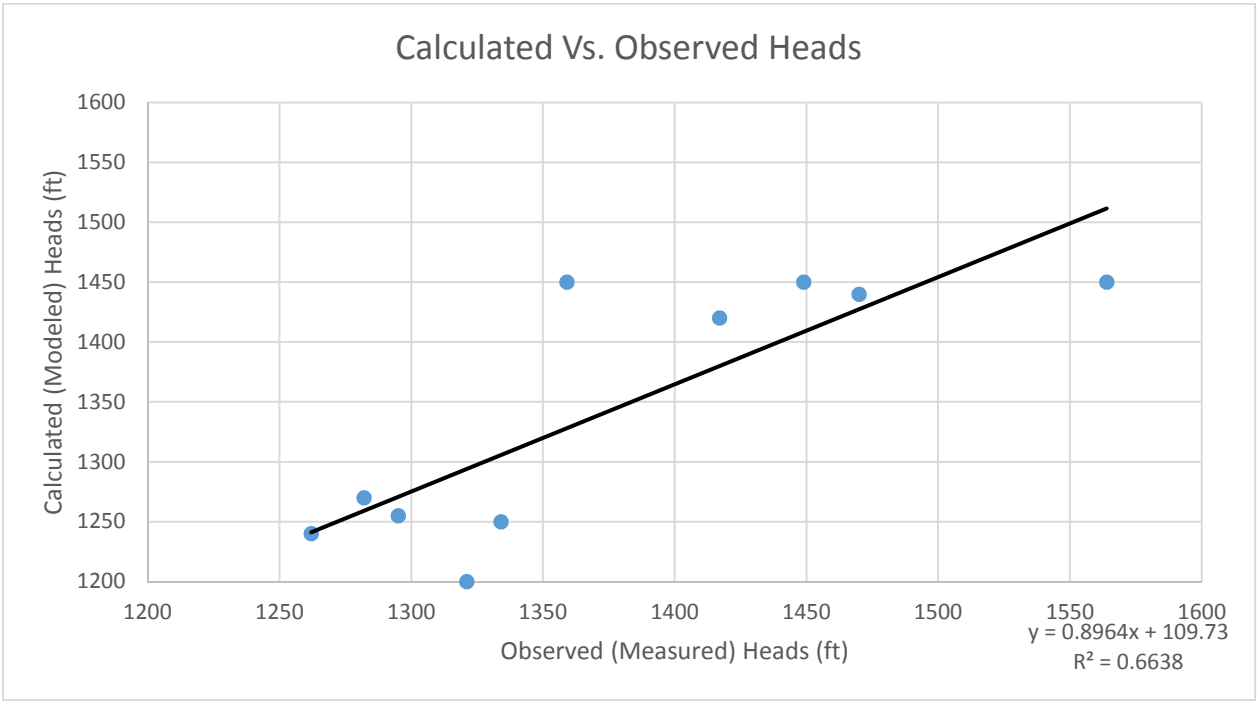

Figure 28: Sensitivity Analysis Linear Regression of Observed vs Calculated Heads for High Conductivity, Layer 1, 3.5E-04 to 3.5E-10 ($\frac{ft}{s}$)

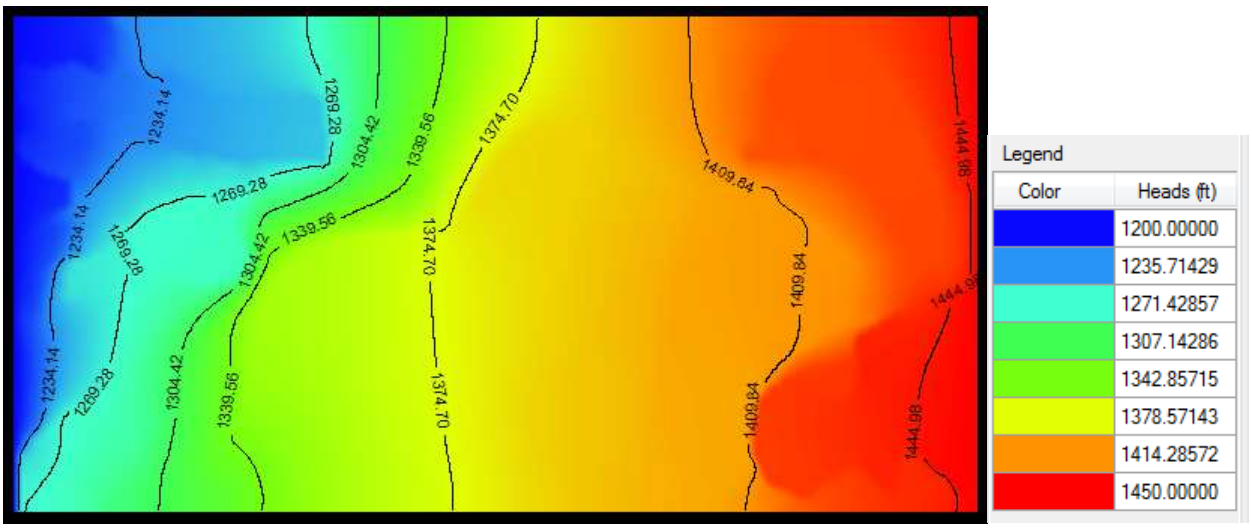

Figure 29: Sensitivity Analysis Low Values, Layer 1, 1.5E-04 to 1.5E-10 ($\frac{ft}{s}$)

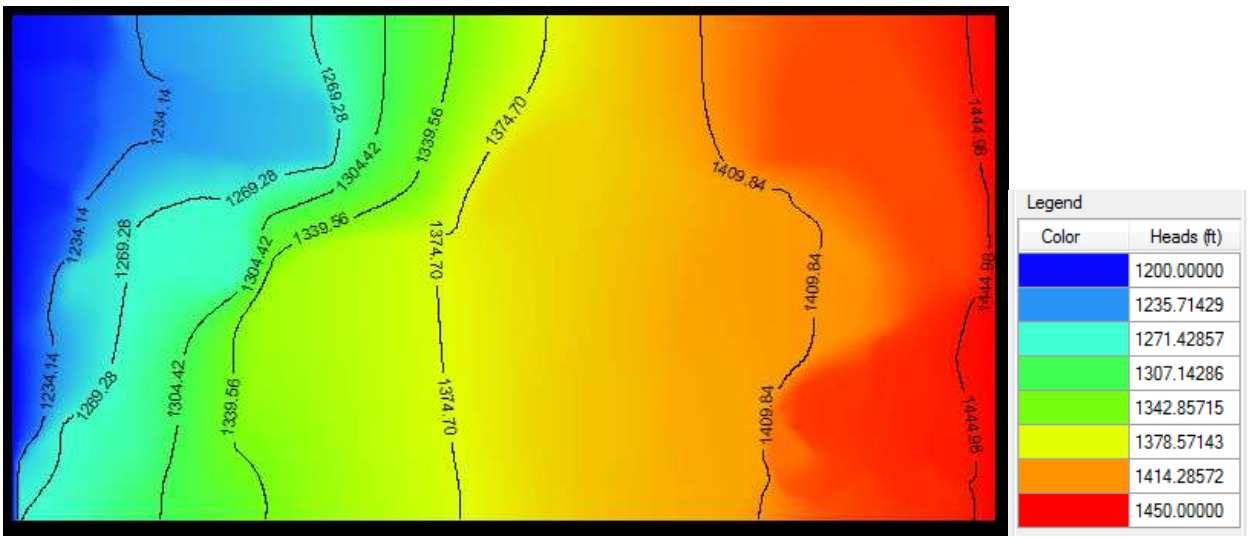

Figure 30: Sensitivity Analysis Low Values, Layer 2, 1.5E-04 to 1.5E-10 ($\frac{ft}{s}$)

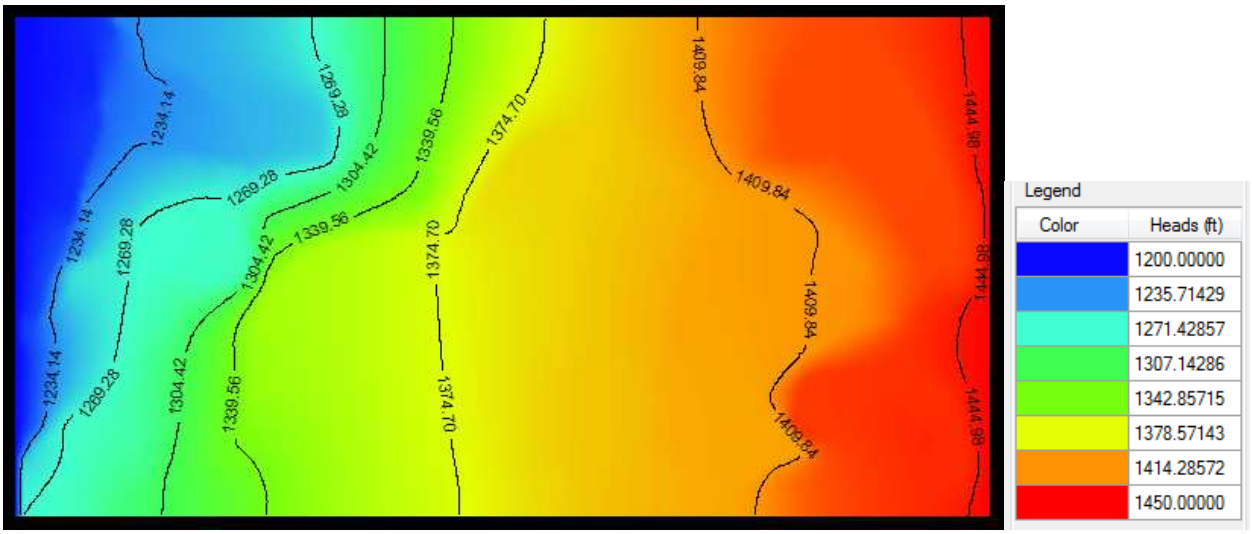

Figure 31: Sensitivity Analysis Low Values, Layer 3, 1.5E-04 to 1.5E-10 ($\frac{ft}{s}$)

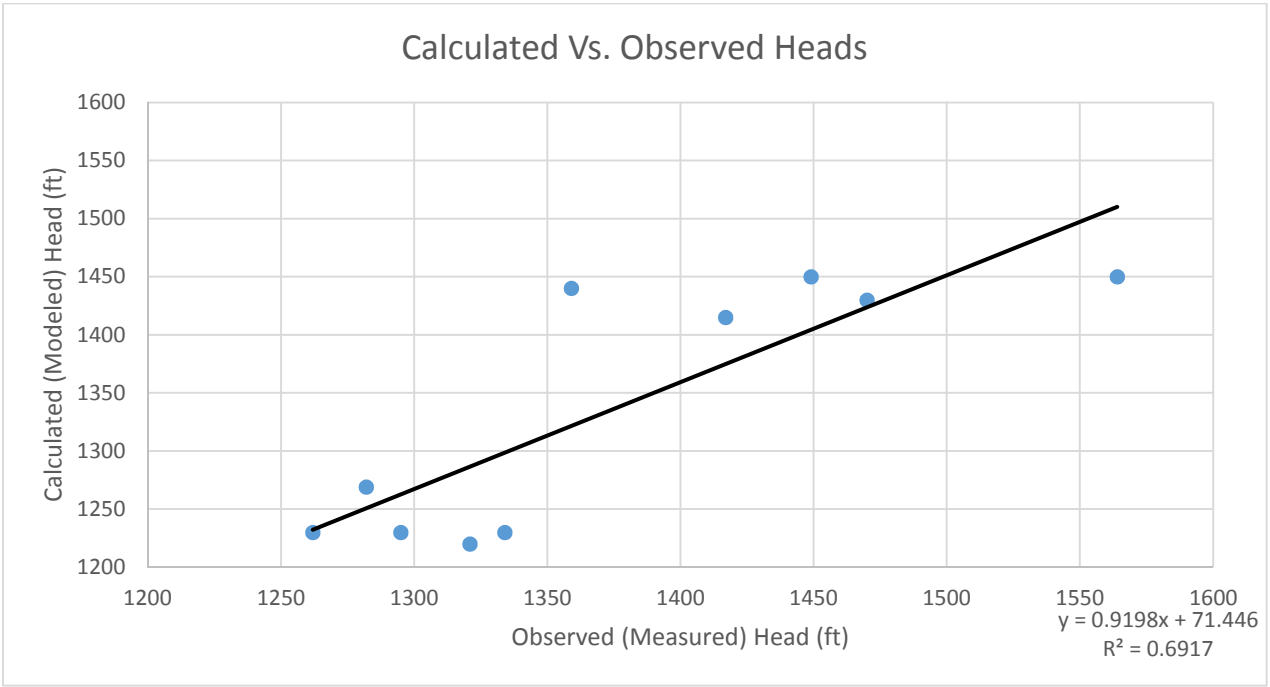

Figure 32: Sensitivity Analysis Linear Regression of Observed vs Calculated Heads for Low Hydraulic Conductivity, Layer 1, 1.5E-04 to 1.5E-10 ($\frac{ft}{s}$)

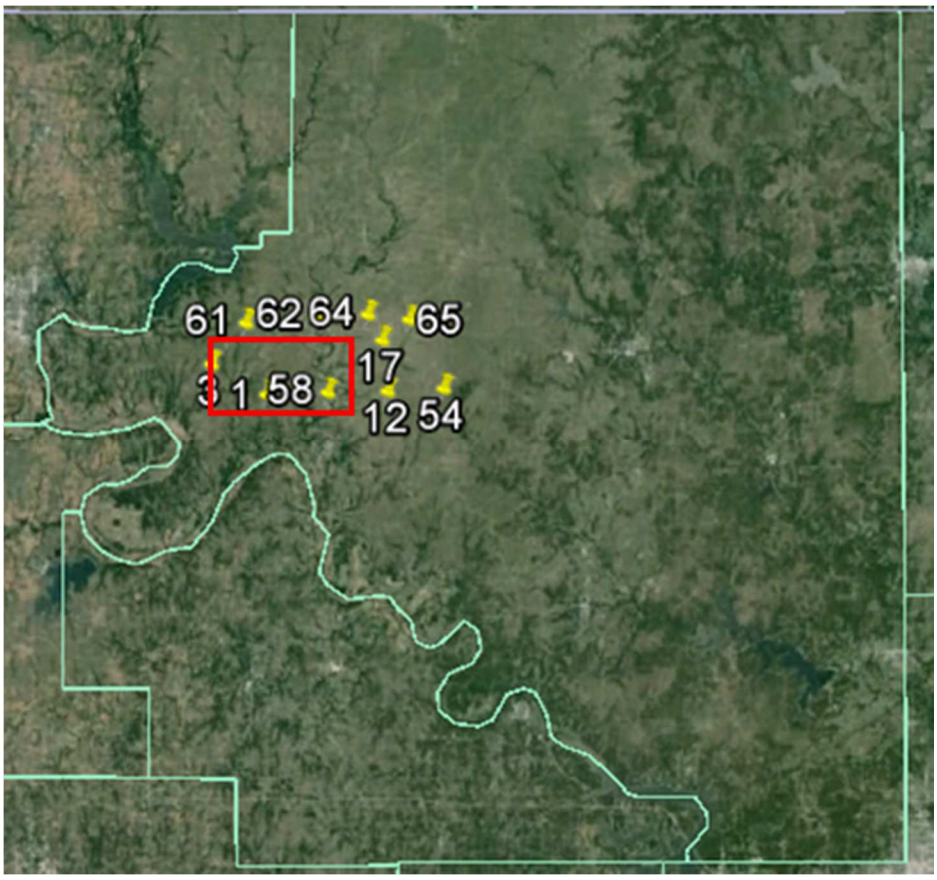

Figure 33: Locations of the drill stem test's hydraulic head values used for the linear regression comparisons for each of the model runs. Locations also used to compare the exact head difference between the calibrated model run and the observed pressure head values (Figure 34).

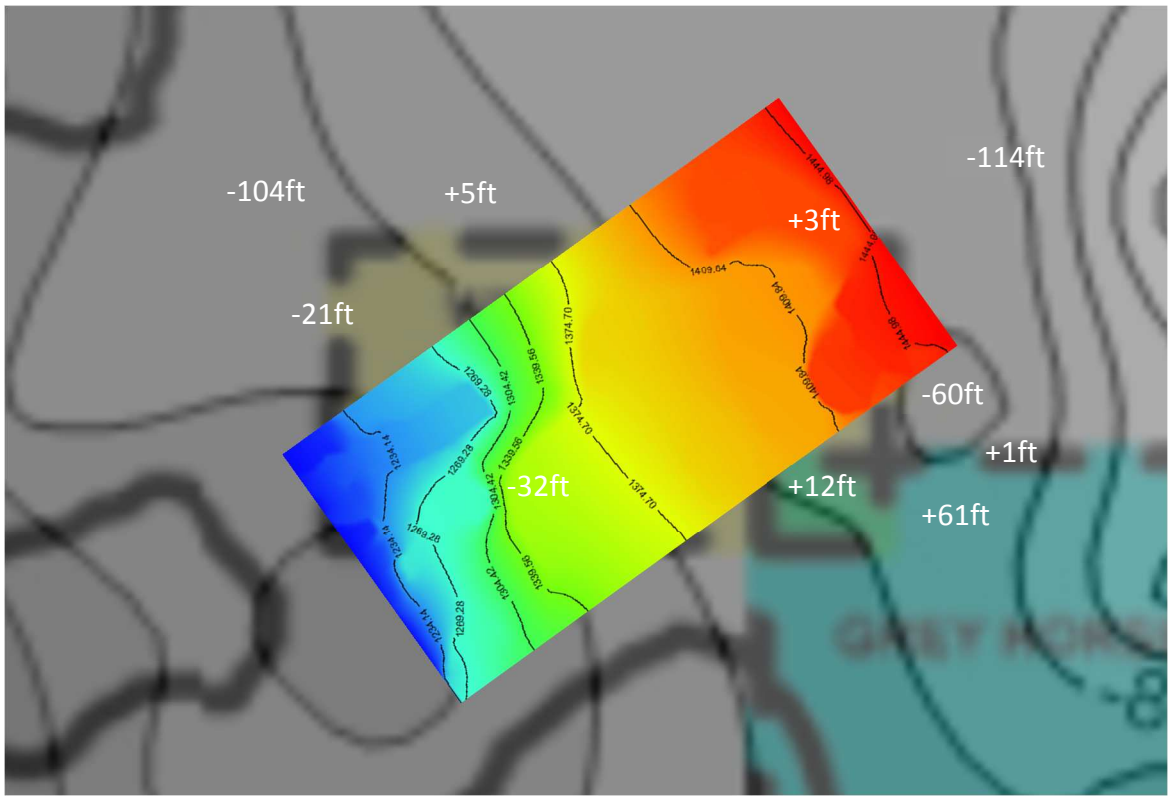

Figure 34: Calibrated model run, layer 1, overlain on the potentiometric surface map, altered to show true geographic similarity. Difference from the observed hydraulic heads and the calibrated model run hydraulic heads, in feet, shown in white. Same locations as the linear regressions used.

In figure 34, the calibrated model run layer one, has been positioned to where the constant head boundaries are parallel to what has been established on the potentiometric surface map, in a NE-SW orientation. The Modflow grid layout is oriented parallel to the primary flow direction to facilitate boundary conditions, in this case, constant head boundaries established to force a gradient from the northeast to the southwest across the model. In addition, to visually and analytically understand the differences between the observed hydraulic heads and the calibrated model run hydraulic heads, the differences were plotted at the geographic locations of each

respective well, that were also used for the linear regressions. In doing so it is shown that the model more closely resembled the hydraulic heads closer to the

Wild Creek seismic survey area and the differences become more extreme where the hydraulic head values had to be interpreted based on the layout of the model.

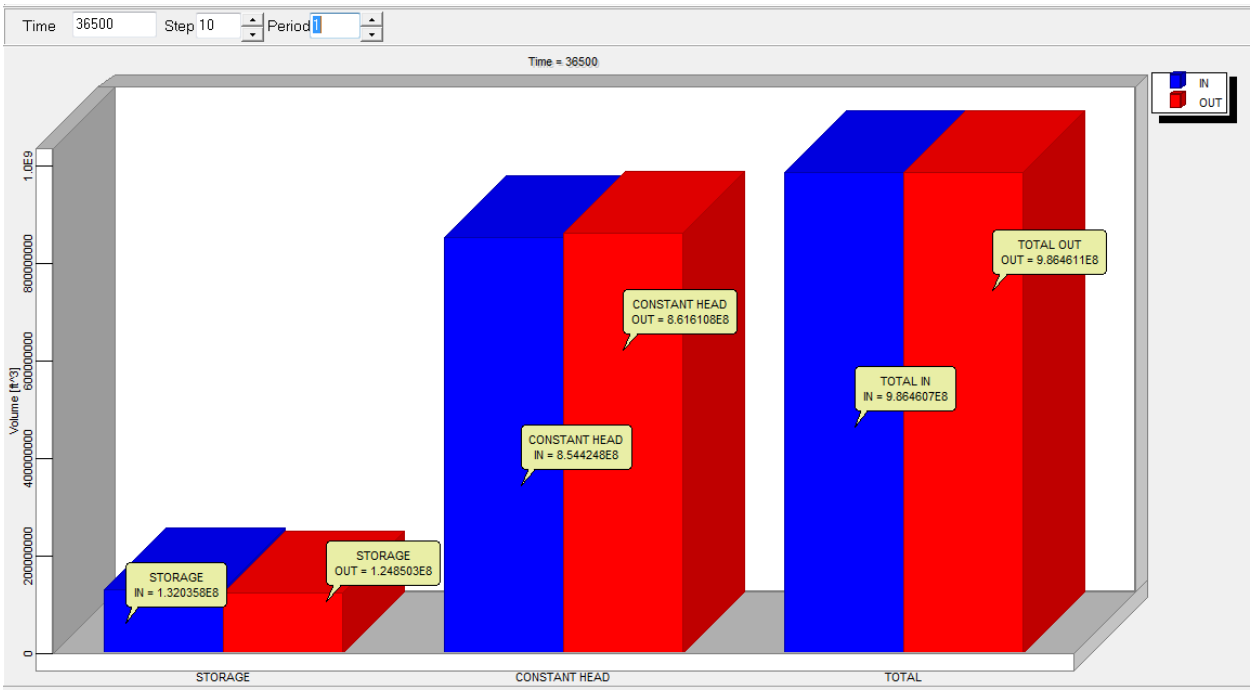

Figure 35: Flow terms in $\frac{ft^3}{100\ years}$ using the calibrated model run as initial heads to run in transient for 100 years (36500 days).

To understand the area's capacities for total water volume flowing through the system for a specified amount of time and to be able to use those flow terms to calculate an average hydraulic conductivity and average velocity across the model domain, a transient run model was created using the calibrated model run head values as the initial starting heads for a transient model run of 100 years. The resulting hydraulic head maps do not change from the calibrated model runs, due to the model setup not being changed, however it does allow for outputs of the flow terms including storage values, constant head values, and the total discharge in and out of

the system. Using the discharge value of 23, 605 (ft^3/day), the total length of the model area, the square footage of the model area, and the change in elevation across the model domain from the east to the west, an average hydraulic conductivity for the entire model domain was calculated to be 0.6295 feet per day or $7.3\ x\ 10^{-6}$ feet per second. This hydraulic conductivity falls in the mid-range of the tabulated data from Freeze and Cherry (1979) that were used for the models. However, this could also mean that within the Wild Creek domain there could be areas of highly karstic areas where the fluid flow is considerable faster, indicating portions of smaller conduit type flow. In addition, using the discharge in feet per day and the calculated average hydraulic conductivity in feet per day, the average velocity across the model domain is 0.01987 feet per day and the time in years for the recharge from 125 miles east to reach this zone is around 91,000 years, using 0.2% porosity and a gradient of 25 feet per mile. This indicates that much of the water in the system was emplaced during the last several glacial/interglacial cycles.

Relevant Equations:

$$\frac{Q}{A} = -K\left(\frac{\Delta h}{\Delta L}\right)$$

Q = Discharge (ft^3/day)

A = Area (ft^2)

$\frac{\Delta h}{\Delta L}$ = Change in hydraulic head ÷ Length of area for change of hydraulic head

$$v = -\frac{K}{n}\left(\frac{\Delta h}{\Delta L}\right)$$

v = Velocity

$-\frac{K}{n}$ = (Hydraulic conductivity ÷ porosity)

$\frac{\Delta h}{\Delta L}$ = Change in hydraulic head ÷ Length of area for change of hydraulic head

VI. Conclusion

Assembling of the data from the drill stem tests, the seismic data, and the well logs permitted for the creation of the seismic amplitude maps, cross-section, potentiometric map, and the Modflow models. Based on these data a groundwater flow model of a portion of the Mississippian system in Osage County, Oklahoma was created, calibrated and run to reproduce a potentiometric surface which was compared to the observed data calculated from the drill stem tests.

In objective 1, the seismic amplitude maps provided a mechanism for estimating hydraulic conductivity spatially across the domain. Once these values were input into the model, there was a small range of hydraulic conductivities that were acceptable for producing model convergence to the predetermined closure criteria (0.001 feet). The sensitivity analysis high and low ranges are included, within the range reported the model produced reliable results, with the closest to observed hydraulic heads being the calibrated model run using the values estimated based on ranges assigned based on tabular data from Freeze and Cherry (1979). The model would not converge for hydraulic conductivity values outside of those indicated in the sensitivity analysis, even when the closure criteria was relaxed to 1 foot. The potentiometric surface map (objective 2) was essential in the creation of the model, but also to have a reliable source for comparison for the model outputs. As shown in the linear regression of the calibrated model run, the hydraulic head values are consistent to the potentiometric surface, demonstrating the methods used are dependable for the creation of further models for this system. In object 3, the structural cross-section accurately generated a basis to create the block and grid setup within the model

domain. Depth, thickness, and the relation to the potentiometric surface was essential for the model setup. For the final objective, all of the previous data were utilized to create the two sensitivity analysis and the calibrated model run. As stated before, the output from the model closely followed the observed hydraulic head values from the potentiometric surface map as seen with the linear regression of the observed vs modeled heads, demonstrating a reliable output, given sufficient detail of the input parameters.

To accurately define the zones of higher porosity and permeability for a spatially larger understanding of the systems characteristics and controls, further data will need to be acquired to create a bigger zone of known parameters for modelling. Specifically, more seismic data will be needed to create a larger array of seismic amplitude maps from which the hydraulic conductivities values can be estimated. With the Wild Creek survey, it was shown that a reliable output can be created, however due to the size of 10 x 5 miles, the model is not spatially broad enough to make a conclusion on the structural controls of the entire system in this geographic area. However, using these methods to create the data parameters, one could successfully create a spatially larger model, utilizing more seismic surveys, to accurately describe this systems controls on porosity and permeability and hence, the reservoir flow capabilities and quantities for the entirety of Osage County, Oklahoma.

VII. References

Bass, N., 1940. Subsurface Geology and Oil and Gas Resources of Osage County, Oklahoma, Part 11. Summary of Subsurface Geology with Special Reference to Oil and Gas, p.380-382

Blakey, R., 2009. Paleogeography and Geologic Evolution of North America: Images that Track the Ancient Landscapes of North America. http://jan.ucc.nau.edu/rcb7/nam.html

Dowdell, B., Roy, A., and Marfurt, K., 2012. An Integrated Study of a Mississippian Tripolitic Chert Reservoir – Osage County, Oklahoma, USA, SEG Las Vegas 2012 Annual Meeting, p.1-5

Evans, C. and Newell, D., 2013. The Mississippian Limestone Play in Kansas: Oil and Gas in a Complex Geologic Setting, Kansas Geological Survey, Public Information Circular 33, p.1-5

Freeze, R.A., and Cherry, J.A., 1979, Groundwater: Englewood Cliffs, NJ, Prentice-Hall, p. 27-29

Johnson, K., 2008. Geologic History of Oklahoma, Oklahoma Geologic Survey, Educational Publication 9:2008, p.3-9

Leach, D., Rowan, L., 1986. Genetic Link Between Ouachita Foldbelt Tectonism and the Mississippi Valley-type Lead-Zinc Deposits of the Ozarks, Geology, V. 14, p.931-935

Mazzullo, 2011. Mississippian Oil Reservoirs in the Southern Midcontinent: New Exploration Concepts for a Mature Reservoir, Search and Discovery AAPG Article #10373 (2011) Posted November 28, 2011

Mazzullo, S., Boardman, D., Godwin, C., and Morris, B., 2013. Revisions of Outcrop Lithostratigraphic Nomenclature in the Lower to Middle Mississippian Subsystem (Kinderhookian to Basal Meremecian Series) Along the Shelf-Edge in Southwest Missouri, Northwest Arkansas, and Northeast Oklahoma, Oklahoma City Geological Society Shale Shaker, v. 63 No.6 p.414-454

McKnight, E. and Fischer, F., 1970. Geology and Ore Deposits of the Picher Field Oklahoma and Kansas, Geological Survey Professional Paper 588, A Discussion of one of the World's Great Mining Fields – its Geology, Mining History, and Potential, p.19-52

Nelson, K.D., et al., 1982. COCORP Seismic Reflection Profiling in the Ouachita Mountains of Western Arkansas: Geometry and Geologic Interpretations: Tectonics, V. 1, p.413-430

Poole, Forest, Perry, Madrid and Amaya-Martínez, 2005, Tectonic synthesis of the Ouachita-Marathon-Sonora orogenic margin of southern Laurentia: Stratigraphic and structural implications for timing of deformational events and plate-tectonic model, GSA Special Papers 2005, v. 393, p. 543-596

Rice, D. D., Finn, T.M., and Hatch, J.R.,1995, Illinois Basin Province (064), Geologic Framework and Description of Coalbed Gas Play, p. 8-10

Rogers, S., 2001. Deposition and Diagenesis of Mississippian Chat Reservoirs, north-central Oklahoma, AAPG Bulletin, v. 85, No.1, p.115-129

Viele, G.W., 1979. Geologic Map and Cross Section, Easter Ouachita Mountains, Arkansas, Geological Society of America Map and Chart Series MC-28F, scale 1:250,000

Watney, W., Guy, W., and Byrnes, A., 2001. Characterization of the Mississippian Chat in the south-central Kansas, AAPG Bulletin, v.85, No.1., p. 85-113